IEEE Access
Multidisciplinary | Rapid Review | Open Access Journal

Received January 15, 2020, accepted February 21, 2020, date of publication March 3, 2020, date of current version March 19, 2020.

Digital Object Identifier 10.1109/ACCESS.2020.2977949

An Analytic Latency Model for a Next-Hop Data-Ferrying Swarm on Random Geometric Graphs

BRADLEY FRASER[1,2], ANDREW COYLE[3], ROBERT HUNJET[4], AND CLAUDIA SZABO[5]

[1]Teletraffic Research Centre, The University of Adelaide, Adelaide, SA 5005, Australia
[2]Aerospace Division, Defence Science and Technology Group, Edinburgh, SA 5111, Australia
[3]Centre for Defence Communications Information Networking, The University of Adelaide, Adelaide, SA 5005, Australia
[4]Land Division, Defence Science and Technology Group, Edinburgh, SA 5111, Australia
[5]School of Computer Science, The University of Adelaide, Adelaide, SA 5005, Australia

Corresponding author: Bradley Fraser (bradley.fraser@dst.defence.gov.au)

This work was supported in part by the Trusted Autonomous Systems Strategic Research Initiative of the Australian Defence Science and Technology Group.

ABSTRACT Next-hop data-ferrying is a data-driven approach to ferrying data between graph components of a disconnected network. In contrast to pre-planned routing methods like the Traveling Salesman tour, only the next-hop is planned, allowing the ferry to be reactive to the data flows within the network. When multiple ferries are used, explicit coordination between them is difficult due to the data-driven approach of the algorithm, and the distributed and disconnected nature of the problem. However, coordinated behavior can still be produced through swarm intelligent means and while this is a useful pragmatic result, mathematical models describing system properties are difficult to develop. This generally results in algorithm correctness being demonstrated through simulation. In this article, we describe the development of a mathematical model of such a next-hop ferrying swarm. We show that the closed-form expression for user data latency is a close match to simulation results for Random Geometric Graphs under the assumption of a zero expected degree. In non-zero degree graphs, a near constant offset between the model and simulation is observed.

INDEX TERMS Data ferrying, emergent behavior, MANET, random geometric graph.

I. INTRODUCTION

Uninhabited Aerial Systems (UAS) are an ideal platform to support user communication networks. Their capability to move freely and in some cases hover, coupled with the capacity to carry communication payloads, affords the quick and easy deployment of additional network nodes; all while enjoying a free-space propagation environment. With the addition of intelligent agents in control of platforms, the autonomous use of such communication assets is a viable path for enhancing user communications. For example, in managed networks, autonomous UAS have been proposed as roaming base stations to alleviate path loss issues in millimeter wave networks [2]; while in the mobile ad-hoc network (MANET) space [3], they have been proposed to provide communications networks in humanitarian assistance and disaster relief (HADR) efforts [4]–[6] as well as providing range-extension [7]–[9] and data-ferrying [10]–[12] services in tactical military networks.

Range extension and data ferrying services both address the problem of degraded user communications but are aimed at different network connectivity situations. Range extension targets semi-disconnected networks where the use of one or more *resource* nodes can be used to reconnect a disconnected graph component, or to provide redundant network paths to remove cut-vertices and bridges within the graph, making it more connected and less vulnerable to individual node losses. Data ferrying on the other hand, is appropriate to situations where end-to-end connectivity cannot be achieved. In this case, resource nodes act as courier pigeons by transferring data between *user* nodes in a delay-tolerant fashion [13]. In this approach, physical proximity is used to overcome signal-to-noise ratio deficits imposed by a hostile radio-frequency (RF) environment and/or large geographic operating areas. Ferry routes can be static such as in Traveling Salesman tours, or dynamic by only planning the next-hop.

The associate editor coordinating the review of this manuscript and approving it for publication was Murilo S. Baptista.

In both cases, the data latency associated with platform movement dominates that associated with RF transmission and so the use of multiple ferrying platforms is desirable; and as the popularity of UAS continues to grow and the enabling-technology decreases in cost, the fielding of platforms en masse is becoming feasible. However, HADR and military applications will likely require distributed and decentralized control, and with many interacting entities, the system becomes a complex multi-agent system that must cooperate to achieve the desired outcome. Furthermore, the multi-hopping of local state information around the network to produce a global state picture is not a scalable approach. Even if it were, agents are not guaranteed to always be in contact with each other, further introducing the problems of information freshness and dissemination. Fortunately, distributed control can be achieved using the principles of swarm intelligence and emergent behavior. While the term 'swarm' has been used to refer to a collection of (many) objects, we use it here in the context of control.

Swarm intelligence is the collective behavior that can be observed in self-organized systems of many interacting individuals [14]. Nature provides many examples of this emergent phenomenon particularly in social insects [15], but also in larger animals such as in fish schooling and bird flocking where the three local rules of attraction, repulsion and cohesion between neighbors produce a remarkably good model for such behavior [16], [17]. The flocking behavior itself is a system-level property, as are all emergent properties, that is not present in individuals themselves. This type of control is distributed, redundant to loss and local. But for the same reasons that make swarms attractive, they also make it difficult to analyze outside of simulation.

To assist with the understanding of how to develop swarm models of wireless telecommunication networks, in this article we describe the development of a mathematical model of an adaptive swarm intelligent resource node system. The algorithm, based on next-hop ferrying, is capable (although not guaranteed) of finding relaying solutions if the topology permits. Inspired by statistical mechanics techniques, observations of emergent structure in the resource node movement at different levels of node density are used as the basis of the model. We then discuss how node density affords the development of emergent behavior (or not) by facilitating agent interactions and look for phase changes in the latency response of the system as resource node entropy decreases.

Hybrid analyses such as this that combine traditional network modeling with statistical, complex network techniques will become increasingly important if emergence-driven and self-organizing network engineering become commonplace.

II. RELATED WORK

A. DATA RELAYING

A survivability-oriented network management approach is taken in [18] to range extension where a distributed network algorithm draws a resource node to a particular location based on graph connectivity metrics. It addresses the problem of making a network harder to break by creating redundant paths. In the distributed approach, raw network state information about a node and it neighbours within a specified hop-count is broadcast to neighbours. Each node then builds up a picture of its local topology which resource nodes can use to geographically place themselves using optimisation of graph metrics. The approach however does not consider disconnected networks. Both [19] and [20] consider using swarm-based control to place multiple mobile resource nodes such that end-to-end connectivity is maintained in a MANET. They use attractive and repulsive type rules based on user and peer resource node locations to place resources. While resources in our approach use peer locations as destinations, traffic stored in a resource node buffer is the only driver in placing the resource in the network. It does not consider the physical location of peer resource nodes. A more recent range extension algorithm uses network capacity modelling to generate force-based velocity control of individual resources to appropriately deploy an aerial network above a congested ground network [21]. The work uses resource node altitude to control the ground coverage and hence the number of connected users to optimise capacity. Reference [22] examines the effect of self-organising resource nodes on tactical networks utilising current MANET military protocols. Resource nodes position themselves in the network to increase route capacity between user nodes. The study also considers the improvement gained by using directional antenna to reduce interference between transceivers. These works are viable approaches to (multi) resource management to improve communication networks where end-to-end connectivity is achievable but again do not consider disconnected networks.

B. DATA FERRYING

Data ferrying algorithms for sparse networks extend from static planning paths using Traveling Salesman Problem (TSP)-based solutions [23], [24], TSP with Neighborhood solutions [25]–[27], to dynamic planning models where only the next hop is calculated [28]–[32]. In these next-hop models, a value function based on statistics such as the number of buffered packets, combined waiting time of buffered packets and the time since last visit are used as heuristics to calculate the next-hop destination. A similar approach is used in our work to make local next-hop decisions and do not claim novelty in this respect. We are interested in how resource nodes implicitly work together to achieve the data transfer. To assist with this cooperation, the work in [33] allows resource nodes to record its visit time in user nodes so that other resources can make better decisions. However, our work does not use any form of signaling in the resource or user nodes outside of the user data it is tasked with transferring. These heuristic algorithms, while comparable via simulation, do not have mathematical models for latency, making it difficult to predict performance when input variables, such as the number of resource nodes, changes.

C. MODELING OF SWARM SYSTEMS

Even with a complete description of a single agent or robot, its behavior is difficult to discern in a swarm setting due to the high number of agent-agent interactions. Further, these microscopic models often become intractable as swarm numbers increase. Macroscopic models on the other hand describe the collective behavior directly, reducing the number of variables to make it computationally more efficient [34]. Due to the fluctuations in the environment, as well as noise in a robot's sensors and actuators, [34] argues for a probabilistic approach to swarm modeling and derive a macroscopic quantity that describes the fraction of robots in a particular state. Similar probabilistic approaches are also taken in [35]–[37] for self-organized tasks. These probabilistic methods are related to the 'mean-field' model where the spatio-temporal evolution of a stochastic process for each agent can be approximated as a single stochastic process in the limit as the number of agents tends to infinity. These models describe the time evolution of the system with ordinary differential equations, partial differential equations and difference equations depending on time continuity. For a review of swarm systems modeled in this way, see [38]. In contrast to this problem, we do not formulate a system description with the intent of describing its collective motion with time; rather, we model a metric of the swarm application (that is, latency) using observations of a pre-determined swarm system. In [39], it is noted that many swarm models are parameterized or driven by empirical measurements. Our experience is sympathetic to this description where observation of the emergent behavior in the system was used directly in building the model.

III. BACKGROUND

A. RANDOM GEOMETRIC GRAPHS

As originally described by Gilbert, vertices of a Random Geometric Graph (RGG) are generated according to a Poisson point process with vertex pairs being connected via an edge if they fall within a fixed range r [40]. As such, RGGs are a useful tool for the investigation of wireless ad-hoc networks with the communication range of nodes being approximated by a circle of radius r. RGGs with generalized connection functions have also been developed to allow for other communication models [41], but for simplicity, we assume the standard disc model. Further to their usefulness in modeling wireless ad-hoc networks, RGGs have well understood connectivity properties [42]. These mirror some of the properties of tactical networks, and so are also useful in better understanding some properties of these networks.

Since the algorithm in which we are modeling can operate in various connectivity environments, we choose RGGs as the network model and formally introduce the RGG below.

Let $\mathcal{G}(n, r)$ represent a graph with a sequence $\mathcal{U} = \{x_1 \dots x_n\}$ of independent and uniformly distributed points on $[0, 1]^d$, then given a fixed $r > 0$, connect two points if their $\mathcal{L}_p$-distance is at most r. In this article, we are only concerned with two-dimensional results ($d = 2$) and the distance measure is the $\mathcal{L}_2$ Euclidean norm. For graph connectivity analysis, it is convenient to represent the radius r as a function of n, that is, $r = r(n)$ and if D is a random variable representing the degree in $\mathcal{G}$, then the expected degree is given by [42]

$$\mathbb{E}[D] = \pi(n-1)r^2 \sim \pi n r^2. \tag{1}$$

A connectivity threshold occurs at $\mathbb{E}[D] = \ln(n)$ which gives a threshold radius of

$$r_t \sim \sqrt{\frac{\ln(n)}{\pi n}} \tag{2}$$

and holds *almost surely*. That is to say that the probability of this result occurring tends to one as $n \to \infty$. Figure 1 plots a RGG example with $r = 0.1$ and $n = 100$. The expected degree (≈ 3.14) is below the connectivity threshold of $\ln(100) \approx 4.61$ ($r_t \approx 0.12$). On inspecting the distance between components, it is clear that some components could be bridged with a resource node, while others cannot and require ferrying. Of course, any gap can be bridged given enough resources. However, this comes at the expense of other components if resources are limited.

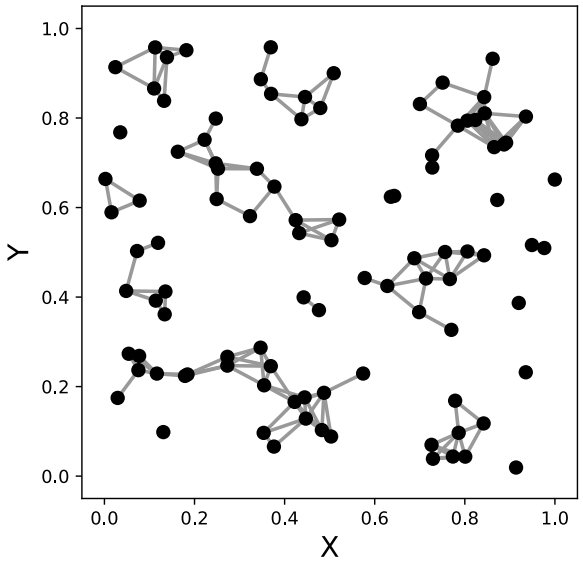

FIGURE 1. A 100 node RGG $r = 0.1$ RGG instantiation.

IV. ADAPTIVE RESOURCE ALGORITHM

We recently introduced an adaptive resource swarm algorithm that is capable of heterogeneous macroscopic emergent behavior dependent on the network connectivity level. The algorithm bridges where possible and ferries where necessary [1]; adaptive to different topologies, number of users and number of resources. However, it is assumed that user node locations are known and are static but global information about other resource node peers is not known nor modeled.

The resource node behavior is defined by several simple rules that govern how the nodes move and how they interact

with other entities. These rules are described below for completeness.

A. RULES

1) RULE 1-RESOURCE NODE NEXT-HOP MOVEMENT DECISION

The next-hop decision rule determines which *user* node a *resource* node should visit next by inspecting its current buffer state. That is, given a set of resource nodes $\mathcal{R}$, then each resource node $i \in \mathcal{R}$ decides on the next user to visit by evaluating the value function

$$v_j = \frac{\sum_{k \in \mathcal{B}_i(j)} w_k}{||x_j - x_i||}, \tag{3}$$

where v_j is the value in visiting user node $j \in \mathcal{U}$, w_k is the waiting time of packet k destined for node j in node i's buffer $\mathcal{B}_i$, x_i is the two-dimensional position vector of node i and $||\cdot||$ is the Euclidean norm. Value functions that inspect traffic buffers are a common approach to next-hop decision making in the data ferrying literature [28]–[32]. Note that finding the optimal value function is out of scope of the article and the reader is directed to the references for investigations of this nature.

Since this control rule is data-driven, only those nodes that are packet destinations will be visited. This can be rectified through the additional rule of visiting nodes if a timer expires regardless of its traffic queue. In this work however, we assume at least some traffic is generated for all nodes. This is a reasonable assumption in, for example, tactical military networks, where the primary purpose is to ensure Position Location Information (PLI) of each node is continually disseminated throughout the network.

2) RULE 2-RESOURCE NODE ROUTING

The routing rule describes how nodes interact with each other when they come into communication range; a modified version of geographic routing is used [43], [44]. In geographic routing, data is exchanged between nodes based on their geographical distance to the destination. When choosing the next-hop destination from any connected peers, the neighbor that is closest to the destination is selected. This rule is implemented as part of the adaptive swarming algorithm with a caveat. The recipient node must either be:

1) The final packet destination (or have a route to the destination); or
2) Another resource node (or have a route to another resource node).

This prevents 'black hole' data sinks from forming by only allowing the sending resource node to deliver the packet to the intended recipient or pass it to a peer resource node. While an intermediate user node may be physically closer to the destination, the sending resource node has no guarantee that another resource node exists in the system to continue the delivery.

3) RULE 3-USER NODE ROUTING

User nodes employ the same geographic routing rule but without the black hole caveat. Traffic then builds up in user nodes on the edges of graph components which helps resource nodes to localize their behavior to component gaps. User nodes will also transmit all current packets in their buffer to any connected resource node regardless of distance to the recipient. This solves some edge cases where for example a resource node would need to approach a solitary user node from the correct direction in order to facilitate traffic flow imposed by the geographic routing.

B. BEHAVIOR

The rules above produce coordinated behavior via stigmergy [45]. In this case, the stigmergic variable is network traffic that, in some sense, acts like a pheromone to guide node behavior. It does this in two ways: firstly, by adding and removing data packets at user nodes, resource nodes communicate or influence which user nodes need visiting at a later time; and secondly, handing off traffic in a geographic way allows resource nodes to operate within their current local area. This produces a seemingly planned behavior where nodes appear to be assigned to different areas. The approach has been shown to be superior to multiple ferries optimally-spaced around an optimal Traveling Salesman Problem tour for various levels of connectivity [1].

It is important to note that stigmergic variables do not convey state information. While it is assumed that user locations are known in advance and are static, resource nodes do not have a better understanding of the network state or the intentions of other resource nodes when data packets are exchanged.

V. MATHEMATICAL MODEL

Swarming systems are often difficult to model mathematically due to the number of individuals and the dynamics involved. Accordingly, in order to model the packet latency of the algorithm we make the simplifying assumption that routing between user nodes is disabled, or equivalently, $\mathbb{E}[D] = 0$. Communication is only allowed between user and resource nodes, and between resource nodes. While this assumption is simply to facilitate model development, such disconnected network topologies may be representative of:

- Extreme RF denial or harsh transmission situations; and
- Situations where nodes only wish to communicate with resource nodes. For example, to save power in wireless sensor networks, or in low detection probability networks.

It is also a conservative assumption, and hence may make sense for allocation of resources.

With the above assumption in place we observed that the resource nodes had a tendency to generate a grid-like structure as resource node density increased. As the communication range increases, resource nodes localize to smaller and

smaller operating areas. This is demonstrated Fig. 2. We thus begin by developing a model based on this behavior.

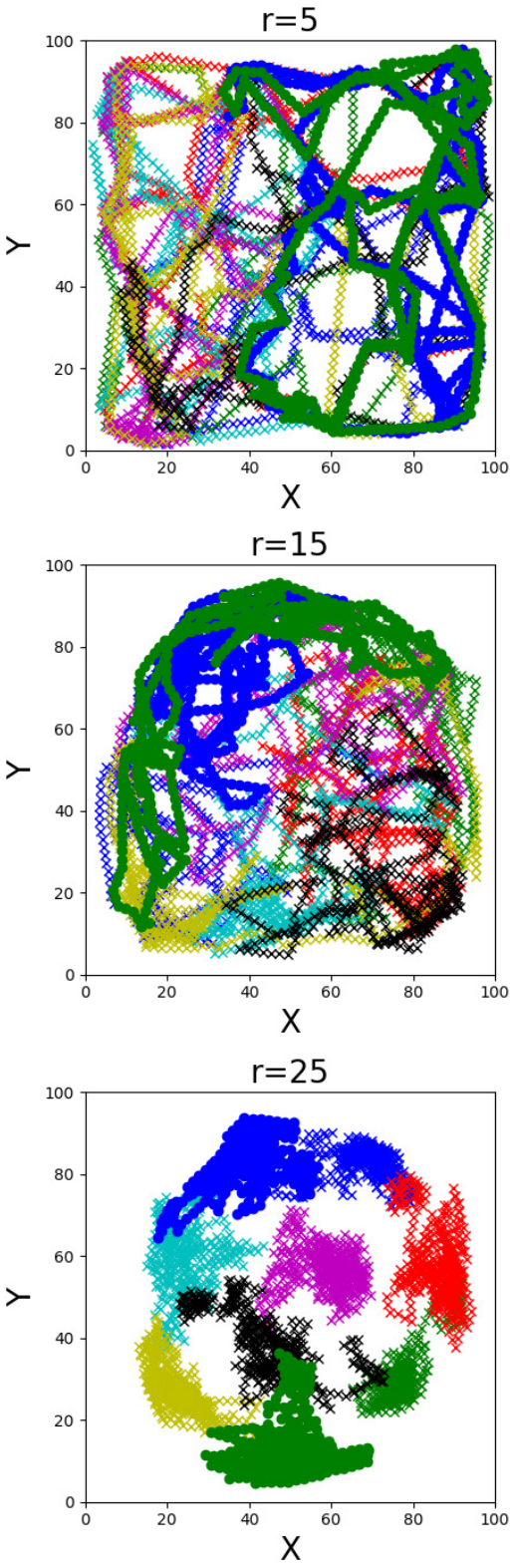

FIGURE 2. Resource node history traces for a 50 user node RGG (not shown) and 9 resource nodes; grid like behavior is generated as resource node range increases (best viewed in color).

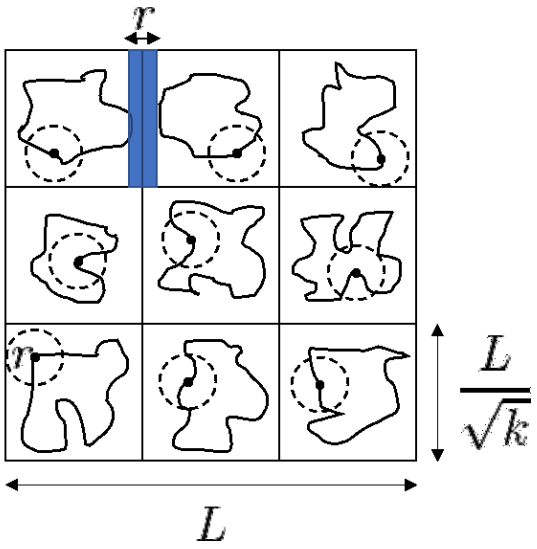

FIGURE 3. The model, a grid of k cells each with their own resource node following a TSP solution with radius r. The blue strip represents a region where adjacent resource nodes can perform a hand-off.

A. INITIAL MODEL

Assume that a RGG of user nodes is divided into a square grid of k cells such that there are $\sqrt{k}$ cells along the grid side. Each cell represents a localized operating area and contains a single resource node as in Fig. 3. Using this grid layout and the assumption that user forwarding is disabled, we develop an analytic expression for the packet delay between user nodes.

1) MEAN WAIT DELAY

We begin by approximating the algorithm behavior within a cell as following a Traveling Salesman Problem (TSP) tour [46]. The current best bounds of an optimal TSP tour $T^*(n)$ on a random set of points in a unit square is given by [47]

$$0.63\sqrt{n} \leq T^*(n) \leq 0.92\sqrt{n} \tag{4}$$

where n is the number of nodes in the unit square. In order to be representative of the typical case, we use the value

$$T^*(n) = 0.70787\sqrt{n} \tag{5}$$

derived from extensive simulation [48]. If there are N total user nodes then there are

$$n_{\text{cell}} = \frac{N}{k} \tag{6}$$

nodes in each cell. Assuming a constant movement speed of one and grid size of L, the mean TSP time, or cell time, is given by

$$t_{\text{cell}} = 0.70787\sqrt{n_{\text{cell}}}\frac{L}{\sqrt{k}}. \tag{7}$$

If r is the radius of the communications range, the ratio of the resource node coverage area to its cell is given by

$$A_c = \frac{\pi r^2}{\left(\frac{L}{\sqrt{k}}\right)^2} = \frac{\pi r^2 k}{L^2} \tag{8}$$

where $0 < A_c \leq 1$. We approximate the mean time nodes must wait for a resource node to visit as $\frac{t_{\text{cell}}}{2}$ modified by the coverage ratio to give

$$t_{\text{wait}} = \frac{t_{\text{cell}}}{2}(1 - A_c). \tag{9}$$

2) INTERMEDIATE CELL TIME

We now estimate the time packets spend in intermediate cells on their way to their destination cell. Assume that if two resource nodes are within a strip of size

$$\frac{r}{2}\frac{L}{\sqrt{k}} \tag{10}$$

of a cell boundary they can hand-off data to each other. The proportion of this hand-off area per cell (ignoring overlap when there is more than one hand-off edge) is

$$A_h = \frac{\frac{rL}{2\sqrt{k}}}{\left(\frac{L}{\sqrt{k}}\right)^2} = \frac{r\sqrt{k}}{2L}, \tag{11}$$

and the mean number of hand-off edges in a grid (cells can have 2 to 4 hand-off edges depending on their location within the grid) is given by

$$h = \frac{4(\sqrt{k} - 1)}{\sqrt{k}}. \tag{12}$$

Therefore the hand-off area ratio is

$$h_r = A_h h \tag{13}$$

where $0 < h_r \leq 1$. The approximate intermediate cell time is then

$$t_{\text{intermediate}} = \frac{t_{\text{cell}}}{2}(1 - h_r). \tag{14}$$

3) TRANSFER TIME

In order to estimate the time taken for a packet to reach its destination cell, we must estimate the number of resource node hand-offs (or number of intermediate cells traversed). Assuming a uniform-random traffic distribution, the probability that no steps between cells is required because the source and destination are in the same cell is

$$p_{\text{no steps}} = \frac{n_{\text{cell}}}{N} \tag{15}$$

where $0 \leq p_{\text{no steps}} \leq 1$. Further assuming shortest-path Manhattan routing between cells, we require the number of steps between cells for data to reach their destination. Consider that along one dimension of the grid there are $(\sqrt{k} - 1)$ unit-length paths, $(\sqrt{k} - 2)$ two-unit length paths, etc. Then in two dimensions, the combined path length is

$$\sum_{i=1}^{\sqrt{k}-1} 2i(\sqrt{k} - i). \tag{16}$$

Now, there are k possible source to destination cell pairs, of which $k - \sqrt{k}$ have a path that is greater than one (source and destination are not in the same cell), so the mean cell path length is

$$\frac{1}{k - \sqrt{k}} \sum_{i=1}^{\sqrt{k}-1} 2i(\sqrt{k} - i) = \frac{\sqrt{k} + 1}{3}. \tag{17}$$

Accounting for the no step probability, the mean number of cell steps required to reach the destination cell is then

$$s = \left(1 - p_{\text{no steps}}\right)\frac{\sqrt{k} + 1}{3}. \tag{18}$$

To calculate a transfer time we use this result and $t_{\text{intermediate}}$ to get

$$t_{\text{transfer}} = t_{\text{intermediate}}(1 + 2s). \tag{19}$$

4) LATENCY

Finally, the latency is given by

$$t_{\text{latency}} = t_{\text{wait}} + t_{\text{transfer}}. \tag{20}$$

Note that in the special case of $k = 1$, $t_{\text{latency}} \approx t_{\text{cell}}$ where on average packets wait half the TSP length to be picked up and then spend another half of the TSP length being delivered.

This model produces a reasonable estimate for data latency (not shown) but is limited to the high-density case where resources nodes form a well-structured grid. To make the model applicable to low-density cases too, several improvements must be made.

B. MODEL IMPROVEMENTS

The modeling of swarms as physical particles is a useful approach as it provides a statistical approximation of the collective and is scalable with the swarm population size. There are also many theories from the physical sciences from which models can been drawn; for example: from active matter [49], fluid dynamics [50], matter states [51], and general chemical kinetics [52].

As our problem centers on agent interaction, models of particle collisions are of interest. Rather than trying to estimate resource node hand-offs through the calculation of hand-off edges and opportunities, we can interpret these particle collisions as hand-offs. We first demonstrate how particle collisions can be modeled using statistical mechanics methods and then apply this idea to the system model.

1) COLLISION RATE

A well-known approach to deriving the collision rate in a gas is by using the following conceptual equation [53]

$$\frac{(\text{collisional volume})(\text{density})}{(\text{time delta})}. \tag{21}$$

In three dimensions, a cylindrical volume with a cross-sectional radius of $2r$ where r is the radius of the gas particle is prescribed. The length of the cylinder is simply the particle speed multiplied by the time delta over which the rate is being measured. Any other particle whose origin lies within the cylinder will cause a collision. The density part of the

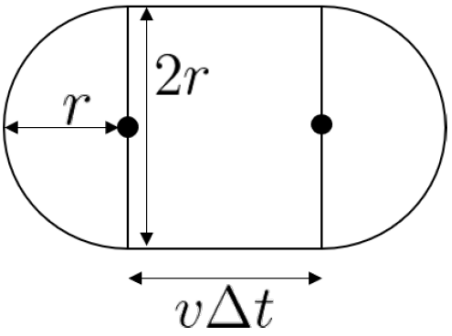

FIGURE 4. The collisional area for a single particle of radius r traveling at velocity v for time Δt. Solid circles represent the starting and finishing origins of the particles over the time Δt.

equation is simply the number of particles divided by the containing volume. The time delta over which the rate is measured cancels with that used in the cylinder length if they are chosen to be the same. Applying this approach to our two-dimensional model we obtain the collision rate (or frequency) f_c as

$$f_c = (2r + \pi r^2)\left(\frac{k}{L^2}\right) \tag{22}$$

where r is the communication radius of the k resource nodes and L is the side length of the square operating area. Since gas particles are typically moving at high speeds, the length of the cylinder is quite long leading to a large cylindrical volume and so the semi-sphere caps at the end of the cylinder are usually omitted. In our case where each node moves a distance of 1 in each time step, the collisional area is $2r \times 1 \times 1 = 2r$. However, the combined end-cap area of πr^2 is significant and so is included in the collisional area as in Fig. 4. This collision expression is directly dependent on both the communication radius and the number of resource nodes in the system.

Figure 5 plots the simulated collision rate and the analytic expression for $k = 9$ and $L = 100$. The analytic expression matches reasonably well up until near the saturation point where some nodes continually stay within each other's communication range; analogous to the non-physical case of particles occupying the same physical space. That is, there is not enough space for them to 'bounce' off each other. Just before saturation, the resource nodes form a rough 3×3 grid (see the bottom diagram of Fig. 2). Along one dimension in this arrangement, the combined range could be $4 \times 25 = 100 = L$. However, how far apart they are spaced depends partly on where the user nodes are. For example, in a particular instance, user nodes may not have spawned right at the very edge of both sides of the field in that slice, meaning that the combined range is not required to be 100 to reach all users. This leads to an inflated collision rate since resource nodes continually stay within range of each other.

To use collision rate in our model, we find the number of collisions per length L as in Fig. 6. The collisional area is then $2rL$ and the probability that a collision occurs is $p = \frac{2rL}{L^2} = \frac{2r}{L}$. Given this probability, we can consider all

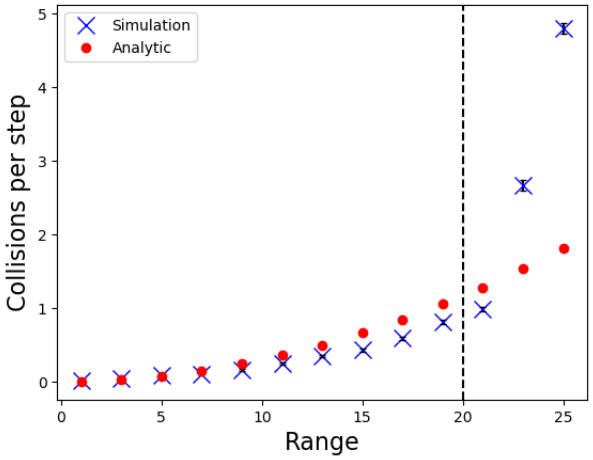

FIGURE 5. Comparison of simulated and analytic collision rate for a system of 9 resource nodes and 50 user nodes with increasing range r.

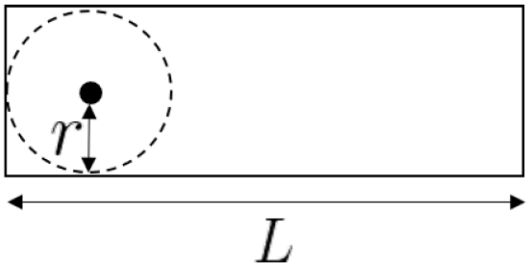

FIGURE 6. The collisional area for the length L.

possible cases of where individual resources may be located; either inside or outside the collisional area. This is approximated using the Binomial distribution as

$$f_c = \sum_{i=1}^{k-1} \min\left(i, \frac{L}{r}\right)\binom{k}{i} p^i (1-p)^{(k-i+1)} \tag{23}$$

where $\min\left(i, \frac{L}{r}\right)$ caps the maximum number of collisions to be the minimum number required to transfer data across the length L given a radius r, and $\binom{a}{b}$ represents the a choose b operation $\frac{a!}{b!(a-b)!}$.

2) EQUIVALENT CELL SIZE

The current model estimates the number of user nodes in each cell by dividing the total number of user nodes by the number of resources. However, in lower density cases, resource nodes travel further around the operating area since the time between collisions is higher. The resource node cells are less well-defined and can overlap. For example, Fig. 7 conceptually shows the operating cells of two nodes, blue and green, shaded in their respective colors. User nodes in the overlapping portion are serviced more often. Note that these cells are not static and the physical area in which they cover changes with time. It is rather the expected coverage at a given time. We denote this expected operating area as the equivalent cell size and estimate it below. Firstly, we can estimate the

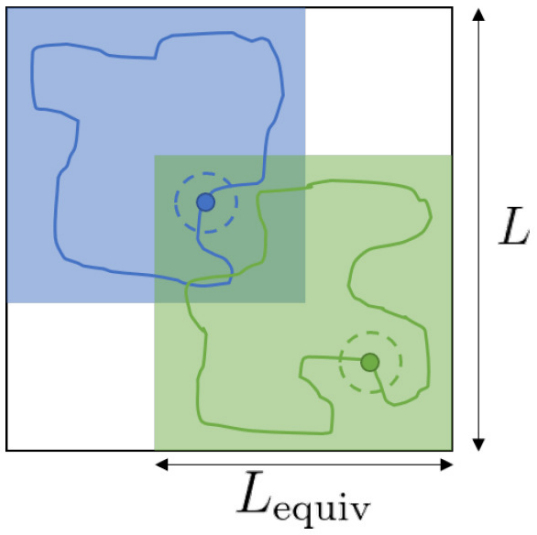

FIGURE 7. A low density case where two resource node cells overlap.

number of resource nodes involved in packet delivery as

$$k_{\text{del}} = 1 + f_c \tag{24}$$

where $1 \leq k_{\text{del}} \leq \sqrt{k}$ since the number of collisions can be considered as the number of hand-offs. The number of user nodes per each cell is then

$$n_{\text{cell}} = \frac{N}{k_{\text{del}}^2}, \tag{25}$$

and the number of resource nodes per cell is

$$k_{\text{cell}} = \frac{n_{\text{cell}} k}{N}. \tag{26}$$

We can now estimate the equivalent cell size a resource node occupies as

$$L_{\text{equiv}} = \frac{L}{k_{\text{del}}} \tag{27}$$

with $0 \leq L_{\text{equiv}} \leq L$. To account for the fact that resource nodes do need to go to the edges of a cell due to their range, we add a correction of $2r$ to give

$$L_{\text{equiv}} = \frac{L}{k_{\text{del}}} - 2r. \tag{28}$$

These new values for n_{cell} and L_{equiv} are used in the calculation of t_{cell} and the mean wait delay is adjusted to be

$$t_{\text{wait}} = \frac{t_{\text{cell}}}{2}\left(1 - \frac{\pi r^2}{L_{\text{equiv}}^2}\right)\frac{1}{k_{\text{cell}}} \tag{29}$$

to account for the fact that a user node may be serviced by multiple resource nodes. The mean length calculated from Manhattan routing is also changed from $\frac{\sqrt{k}+1}{3}$ to $\frac{\sqrt{k_{\text{del}}}+1}{3}$ and $t_{\text{intermediate}} = \frac{t_{\text{cell}}}{2}$.

VI. MODEL PERFORMANCE

To evaluate the model's performance we examine two metrics: the number of resource node hand-offs and overall packet latency. All simulation results were gathered from 5 trials of 2500 iterations using a 50 user node, 100 unit square RGG.

A. RESOURCE NODE HAND-OFFS

Figure 8 plots the number of hand-offs between resource nodes and the number of Manhattan steps calculated in the model. As the communication range increases and the resource nodes become more structured, it becomes easier to estimate hand-offs because cell boundaries are more well defined and the estimation becomes more accurate. As mentioned previously in the particle collision calculation when $r = 25$, the hand-offs plateau after 9 resource nodes since the 3×3 configuration fits into the 100×100 operating area. Extra resources do not help in this situation and the simulation hand-offs begin to vary much more since the extra nodes are still used in the delivery. A similar situation occurs in the $r = 20$ case after 16 resource nodes.

Ignoring unnecessary hand-offs could be a candidate for algorithm optimization, however a better optimization is to have an understanding of how many resources nodes are required to begin with. The latency model was initially developed to understand the marginal benefit of adding additional resource nodes to the system so that optimal team numbers could be devised. This work is ongoing.

We note the larger discrepancy between the model and simulation in the $r = 1$ case and hypothesis that it is due to the correlated nature of the agent movement. That is, more interactions are likely in the simulation since all agents are moving on straight line trajectories between user nodes as opposed to the random trajectories the particle collision model describes. This of course is true for all results but the effect is hidden as the larger ranges begin to dominate the movement.

B. DATA LATENCY

Figure 9 plots the data latency as measured by user nodes and the analytic model. Similarly to the hand-off plots, the model becomes more accurate as the radius increases due to the improved structure in the node movement.

Figure 10 plots the Root Mean Square Error (RMSE) and Mean Absolute Error (MAE) along the resource node number dimension. Interestingly, the curves are very similar indicating that the magnitude of individual errors are roughly consistent since the RMSE is more sensitive to larger deviations [54]. This can be interpreted to mean that the model deviates from the simulation by a (near) constant factor. We note that the model is using an optimal TSP tour to estimate behavior within a cell and the constant deviation may be due to this assumption. We can directly compare the next-hop behavior and the TSP bound in the $r = 1, n = 1$ case

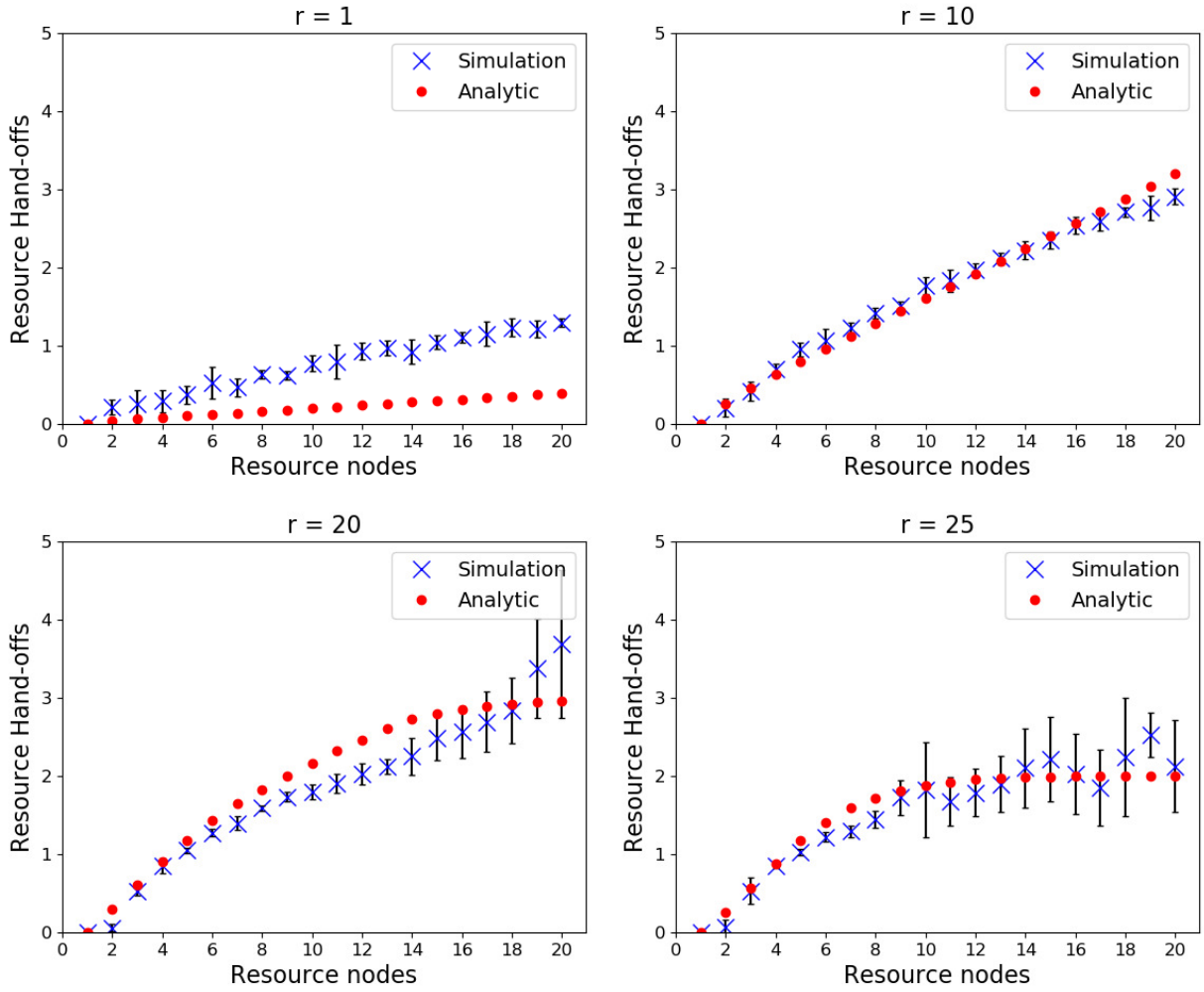

FIGURE 8. Analytic and simulated results for the number of hand-offs between resource nodes. Error bars display a 95% confidence.

where the latency is only approximately 20% longer; an interesting result given the unplanned, next-hop approach.

C. APPLICABILITY TO HIGHER CONNECTIVITY CASES

Initially to build the model, edges between user nodes were ignored to create RGGs with an expected degree of zero. Figure 11 compares the model to simulations where user node routing was allowed, as per the original algorithm. Topologies were tested with $r = \{5, 10, 15, 20\}$, corresponding to $\mathbb{E}[D] = \{0.39, 1.57, 3.53, 6.28\}$ with the connectivity threshold occurring at $\mathbb{E}[D] = 3.91 (r_t \approx 16)$, almost surely. Note that $r = 1$ was not tested since the results are nearly identical to the first simulation.

As expected, the simulation results reveal a lower latency as compared to the fully disconnected case since data can be routed through components of connected user nodes. The magnitude of this effect increases with increasing radius.

The near constant offset between the model and simulation results observed in the fully disconnected case appears to be non-constant here. The curve shapes however are maintained except in the $r = 20$ case which is well beyond the connectivity threshold. Model latency is based on the number of nodes within a cell, however in higher connectivity cases, components containing more than one node effectively appear as a single node due to the routing; something the model cannot account for.

VII. DISCUSSION

In this section we discuss how the model results align with how emergent systems are thought to arise; namely, through the interaction of their constituent members. We also discuss how phase transitions can occur in these systems and look for evidence of those transitions in the latency model.

Emergent behavior is generated through the interaction of individual entities where those interactions can cause the participants to change their state [55]. Thus, in order for the emergent property to form, interactions are necessary. Indeed, studies have characterized how the emergent property breaks down when those interactions are interfered with [56]. The results above demonstrate a similar phenomenon whereby

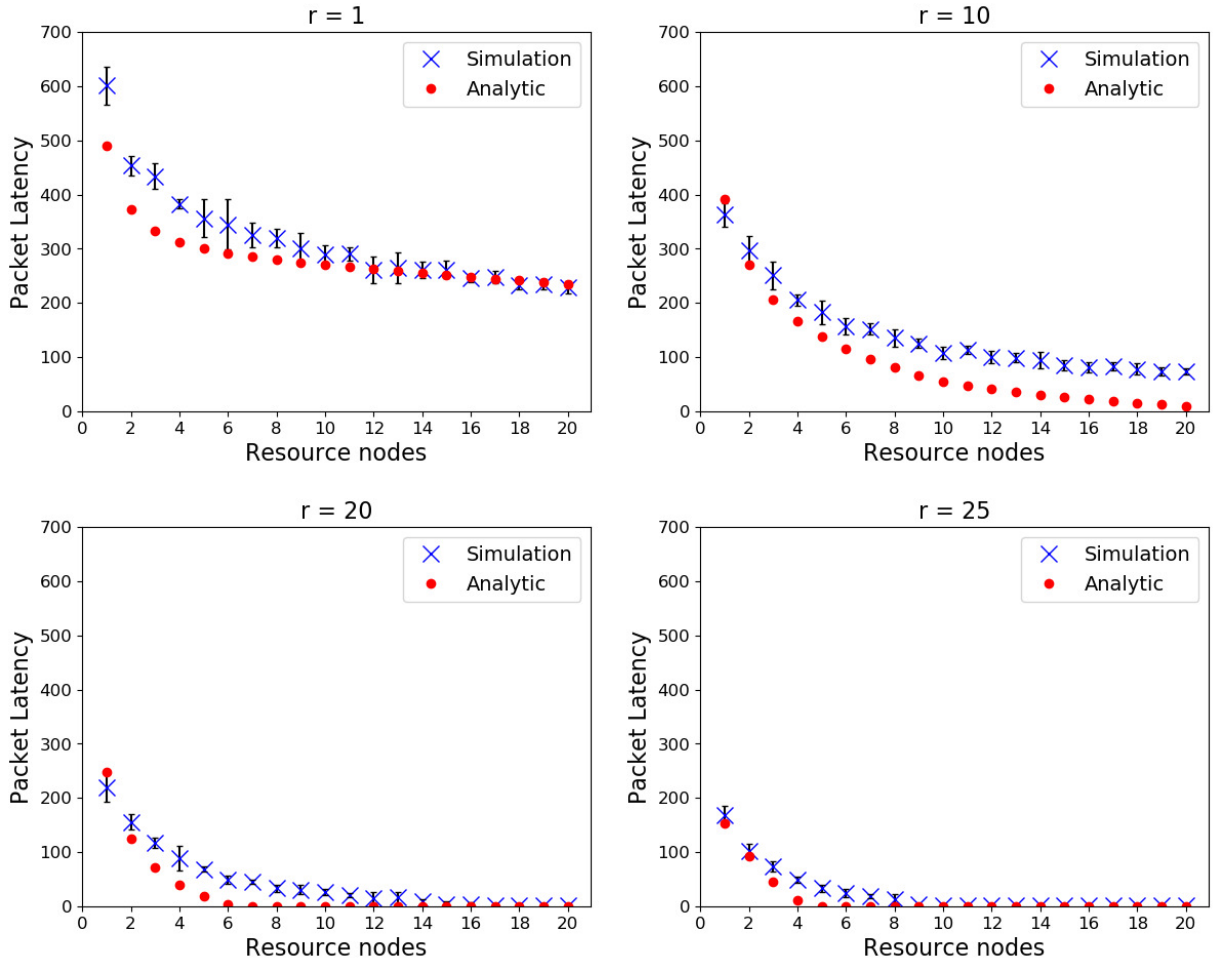

FIGURE 9. Analytic and simulated results for the data latency. Error bars display a 95% confidence.

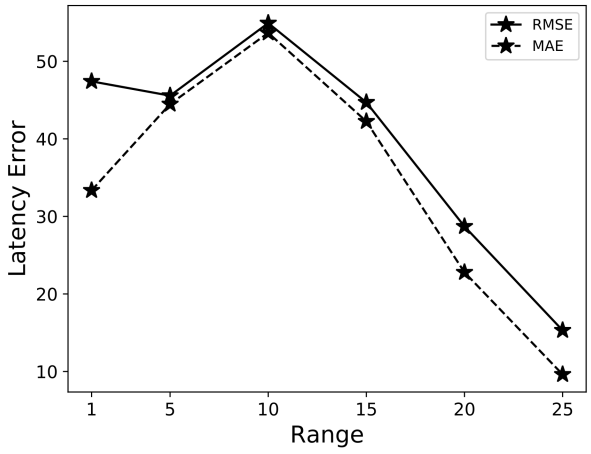

FIGURE 10. Root Mean Square and Mean Absolute Error in the data latency between the model and simulation with increasing range r.

reducing the opportunity for interaction (by reducing the density via range or node numbers) reduces the development of localized resource node behaviour presenting as a less efficient algorithm.

Some systems that exhibit emergent behaviour also contain phase changes whereby the system radically changes as a result of an incremental change in some variable [57]; connectivity in random graphs is one such example [58]. In these graphs, an incremental increase in expected node degree causes the graph to shift from a disconnected to connected state with high probability. Analogously, in our system we examine the incremental increase of resource node range and its effect on latency.

Figure 12 plots the probability of data latency being less than an arbitrarily chosen threshold of 50 time-steps using 9 resource nodes. The 'comms' data set represents the adaptive swarm resource algorithm while the 'no comms' data set represents the same algorithm but with communication between resource nodes having been disabled. In the case where communication ranges are small, there is little opportunity for nodes to interact and the minor improvement in latency with increasing range is simply a consequence of additional coverage. In this regime, the two algorithms are equivalent. As resource nodes begin to interact and self-organize, a phase transition occurs wherein the probability of satisfying the latency threshold dramatically increases.

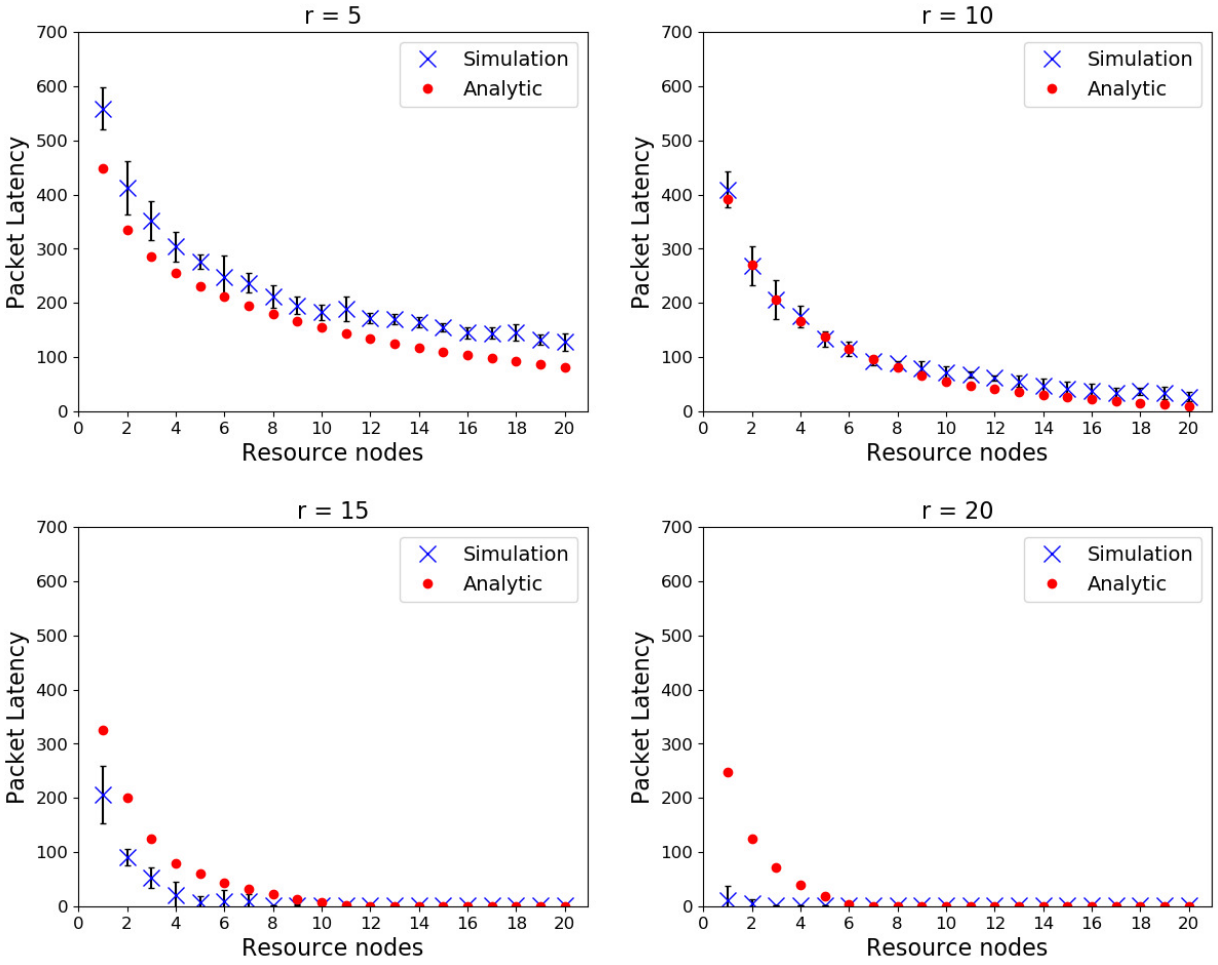

FIGURE 11. Analytic and simulated results for the data latency with user node routing enabled. Error bars display a 95% confidence. Note that we show smaller range values for the connected case since the graph quickly becomes connected at higher ranges.

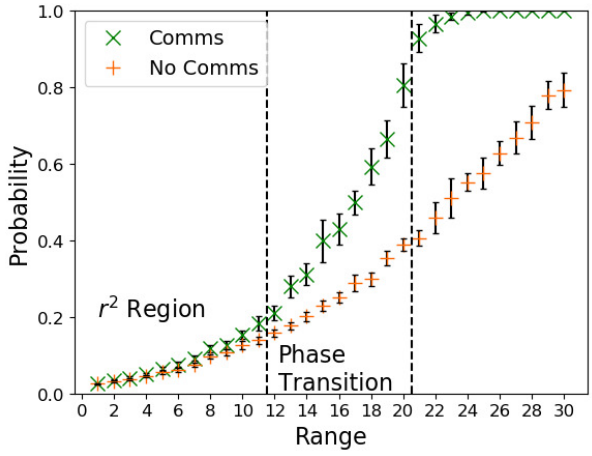

FIGURE 12. A phase transition in the probability of data latency being less than 50 time-steps. Error bars display a 95% confidence.

Phase transitions often exhibit a sigmoid shape (or step function in the extreme case). The adaptive algorithm displays a shape somewhat akin to the sigmoid function. However, given that there are 9 resource nodes and the density is reasonably high (50 user nodes in a 100unit square), it is highly likely that at least one packet would have a latency less than 50, leading to a non-zero probability even for small ranges; altering the shape from a traditional sigmoid. It was found that the lower the chosen threshold, the sharper the phase transition, and a phase transition was not observed in the case without resource node communications. Rather, the curve is simply proportional to r^2 and even with a range of 30 that produces a combined coverage ratio of $9 \times \pi \times 30^2/100^2 \approx 2.5$ times the operating area, the probability is not guaranteed; the nodes are not organized, producing a high coverage overlap between them.

While we have seemingly found a phase transition in the data latency, it is actually a different representation of the phase transition found in the connectivity of the resource node graph. Choosing the latency threshold to be 0 is equivalent to requiring that a path is available to every user node from every user node.[1] This occurs when the resource nodes

[1] Packets are routed instantaneously if a path is available during a time-step in the simulation.

are connected and their combined coverage encompasses all users in the network.

From a practical point of view, we can use these phase transition graphs in system design if they too could be modeled. For example, the range can be chosen such that it meets an acceptably high probability for a given latency; saving transmission power in this case. We hypothesis that a similar curve would be observed when holding range constant and the resource node count is the free variable.

VIII. CONCLUSION

This article describes the mathematical modeling of an adaptive resource swarm algorithm facilitating communications between user nodes on Random Geometric Graphs. Swarm intelligent-based algorithms are difficult to model mathematically due to the number of individuals and the dynamics involved. However, under the assumptions of: uniform traffic distribution and zero graph connectivity; we used observations of emergent structure within resource nodes and statistical mechanics techniques to generate a data latency model that performs well as compared to simulation. This approach to building the model is useful in understanding how to analyze the structure of mass deployments of (Unmanned Aerial System) swarms for coordinated tasks, where that coordination is achieved implicitly through swarm intelligence and emergent behavior.

Phase transitions akin to those seen in connectivity properties of random graphs were observed in the probability of the system meeting a specific latency threshold. The probability rapidly moved from low to high at a critical point as the communications range of resource nodes increased. A non-cooperative, non-emergent version of the algorithm did not display this behavior.

The latency model and analysis of phase transitions gives an indication of the marginal benefit of adding more resource nodes into the system and/or increasing resource node range. Knowing exactly how many nodes to use in swarm systems, and the impact on performance this variable has, is often difficult to quantify. As part of future work, we intend to examine this problem and use the model to optimize the swarm size given specific performance requirements when resource nodes incur a non-zero cost to operate.

ACKNOWLEDGMENT

This work extends, and has been partially published in [1].

REFERENCES

[1] B. Fraser, A. Coyle, C. Szabo, and R. Hunjet, "Adaptive swarm control for mobile resource placement in wireless ad-hoc networks," in *Proc. IEEE 20th Int. Symp. 'World Wireless, Mobile Multimedia Netw.' (WoWMoM)*, Jun. 2019, pp. 1–6.

[2] A. Perez, A. Fouda, and A. S. Ibrahim, "Ray tracing analysis for UAV-assisted integrated access and backhaul millimeter wave networks," in *Proc. IEEE 20th Int. Symp. 'World Wireless, Mobile Multimedia Netw.' (WoWMoM)*, Jun. 2019, pp. 1–5.

[3] C.-K. Toh, *Ad Hoc Mobile Wireless Networks: Protocols and Systems*, 1st ed. Upper Saddle River, NJ, USA: Prentice-Hall, 2002.

[4] S. Hauert, S. Leven, J.-C. Zufferey, and D. Floreano, "Communication-based swarming for flying robots," in *Proc. Workshop Netw. Sci. Syst. Issues Multi-Robot Autonomy, IEEE Int. Conf. Robot. Automat.*, May 2010, pp. 1–4.

[5] R. M. Santos, J. Orozco, D. Mosse, V. Petrucci, S. F. Ochoa, and R. Meseguer, "Flying real-time network for disaster assistance," in *Ubiquitous Computing and Ambient Intelligence* (Lecture Notes in Computer Science). Cham, Switzerland: Springer, Nov. 2017, pp. 591–602.

[6] M. Micheletto, V. Petrucci, R. Santos, J. Orozco, D. Mosse, S. Ochoa, and R. Meseguer, "Flying real-time network to coordinate disaster relief activities in urban areas," *Sensors*, vol. 18, no. 5, p. 1662, May 2018.

[7] M. Elliot and T. Stevens, "Dynamic range extension using HARLEQUIN and HAIL," in *Proc. IEEE Mil. Commun. Conf. (MILCOM)*, Nov. 2016, pp. 835–841.

[8] K.-P. Hui, D. Phillips, and A. Kekirigoda, "Beyond Line-of-Sight range extension with OPAL using autonomous unmanned aerial vehicles," in *Proc. IEEE Mil. Commun. Conf. (MILCOM)*, Oct. 2017, pp. 279–284.

[9] S. M. Al-Shehri, P. Loskot, and M. J. Hirsch, "Enabling connectivity for tactical networks in mountainous areas by aerial relays," *Telecommun. Syst.*, vol. 71, no. 4, pp. 561–575, Aug. 2019.

[10] K. Usbeck, M. Gillen, J. Loyall, A. Gronosky, J. Sterling, R. Kohler, R. Newkirk, and D. Canestrare, "Data ferrying to the tactical edge: A field experiment in exchanging mission plans and intelligence in austere environments," in *Proc. IEEE Mil. Commun. Conf.* Los Alamitos, CA, USA: IEEE Computer Society, Oct. 2014, pp. 1311–1317.

[11] B. Fraser and R. Hunjet, "Data ferrying in tactical networks using swarm intelligence and stigmergic coordination," in *Proc. 26th Int. Telecommun. Netw. Appl. Conf. (ITNAC)*, Dec. 2016, pp. 1–6.

[12] R. Hunjet, B. Fraser, T. Stevens, L. Hodges, K. Mayen, J. C. Barca, M. Cochrane, R. Cannizzaro, and J. L. Palmer, "Data ferrying with swarming UAS in tactical defence networks," in *Proc. IEEE Int. Conf. Robot. Autom. (ICRA)*, May 2018, pp. 6381–6388.

[13] K. Fall, "A delay-tolerant network architecture for challenged Internets," in *Proc. Conf. Appl., Technol., Archit., Protocols Comput. Commun. (SIGCOMM)*. New York, NY, USA: ACM, 2003, pp. 27–34.

[14] E. Bonabeau, M. Dorigo, and G. Theraulaz, *Swarm Intelligence: From Natural to Artificial Systems*. New York, NY, USA: Oxford Univ. Press, 1999.

[15] S. Garnier, J. Gautrais, and G. Theraulaz, "The biological principles of swarm intelligence," *Swarm Intell.*, vol. 1, no. 1, pp. 3–31, Jul. 2007.

[16] C. W. Reynolds, "Flocks, herds and schools: A distributed behavioral model," *ACM SIGGRAPH Comput. Graph.*, vol. 21, no. 4, pp. 25–34, Aug. 1987.

[17] R. Olfati-Saber, "Flocking for multi-agent dynamic systems: Algorithms and theory," *IEEE Trans. Autom. Control*, vol. 51, no. 3, pp. 401–420, Mar. 2006.

[18] K.-P. Hui, P. Pourbeik, P. George, D. Phillips, S. Magrath, and M. Kwiatkowski, "OPAL–a survivability-oriented approach to management of tactical military networks," in *Proc. Mil. Commun. Conf. (MILCOM)*, Nov. 2011, pp. 1127–1132.

[19] A. Konak, G. E. Buchert, and J. Juro, "A flocking-based approach to maintain connectivity in mobile wireless ad hoc networks," *Appl. Soft Comput.*, vol. 13, no. 2, pp. 1284–1291, Feb. 2013.

[20] R. Hunjet, "Autonomy and self-organisation for tactical communications and range extension," in *Proc. Mil. Commun. Inf. Syst. Conf. (MilCIS)*, Nov. 2015, pp. 1–5.

[21] S. Park, K. Kim, H. Kim, and H. Kim, "Formation control algorithm of multi-UAV-based network infrastructure," *Appl. Sci.*, vol. 8, no. 10, p. 1740, Sep. 2018.

[22] A. Coyle, "Using directional antenna in UAVs to enhance tactical communications," in *Proc. Mil. Commun. Inf. Syst. Conf. (MilCIS)*, Nov. 2018, pp. 1–6.

[23] W. Zhao and M. H. Ammar, "Message ferrying: Proactive routing in highly-partitioned wireless ad hoc networks," in *Proc. 9th IEEE Workshop Future Trends Distrib. Comput. Syst. (FTDCS)*, May 2003, pp. 308–314.

[24] W. Zhao, M. Ammar, and E. Zegura, "Controlling the mobility of multiple data transport ferries in a delay-tolerant network," in *Proc. IEEE 24th Annu. Joint Conf. IEEE Comput. Commun. Societies*, vol. 2, Mar. 2005, pp. 1407–1418.

[25] M. M. Bin Tariq, M. Ammar, and E. Zegura, "Message ferry route design for sparse ad hoc networks with mobile nodes," in *Proc. 7th ACM Int. Symp. Mobile Ad Hoc Netw. Comput. (MobiHoc)*. New York, NY, USA: ACM, 2006, pp. 37–48.

[26] R. Sugihara and R. K. Gupta, "Path planning of data mules in sensor networks," *ACM Trans. Sensor Netw.*, vol. 8, no. 1, pp. 1–27, Aug. 2011.
[27] J.-S. Liu, S.-Y. Wu, and K.-M. Chiu, "Path planning of a data mule in wireless sensor network using an improved implementation of clustering-based genetic algorithm," in *Proc. IEEE Symp. Comput. Intell. Control Autom. (CICA)*, Apr. 2013, pp. 30–37.
[28] M. C. Chuah and P. Yang, "A message ferrying scheme with differentiated services," in *Proc. IEEE Mil. Commun. Conf. (MILCOM)*, vols. 1–5. New York, NY, USA: IEEE, Oct. 2005, pp. 1521–1527.
[29] M. C. Chuah and P. Yang, "Performance evaluations of various message ferry scheduling schemes with two traffic classes," in *Proc. 4th IEEE Consum. Commun. Netw. Conf.*, Jan. 2007, pp. 227–233.
[30] J. Peng, J. Liu, and L. Xue, "A multi-constraint ferry routing scheme for delay tolerant networks," in *Proc. 8th Int. Conf. Wireless Commun., Netw. Mobile Comput.* New York, NY, USA: IEEE, Sep. 2012, pp. 1–4.
[31] X. Wu, Y. Chen, M. Xu, and W. Peng, "TAFR: A TTL-aware message ferry scheme in DTN," in *Proc. 4th Int. Conf. Comput. Inf. Sci.*, Aug. 2012, pp. 1380–1383.
[32] T. Simon and A. Mitschele-Thiel, "A self-organized message ferrying algorithm," in *Proc. IEEE 14th Int. Symp. 'World Wireless, Mobile Multimedia Netw.' (WoWMoM)*, Jun. 2013, pp. 1–6.
[33] M. Harounabadi and A. Mitschele-Thiel, "Stigmergic communication for self-organized multi ferry delay tolerant networks," *Mobile Netw. Appl.*, vol. 23, no. 5, pp. 1260–1269, Jan. 2017.
[34] K. Lerman, A. Martinoli, and A. Galstyan, "A review of probabilistic macroscopic models for swarm robotic systems," in *Swarm Robotics*. Berlin, Germany: Springer, 2005, pp. 143–152.
[35] O. Soysal and E. Şahin, "A macroscopic model for self-organized aggregation in swarm robotic systems," in *Swarm Robotics*. Berlin, Germany: Springer, 2007, pp. 27–42.
[36] H. Hamann and H. Wörn, "An analytical and spatial model of foraging in a swarm of robots," in *Swarm Robotics*. Berlin, Germany: Springer, 2007, pp. 43–55.
[37] H. Hamann and H. Wörn, "A framework of space-time continuous models for algorithm design in swarm robotics," *Swarm Intell.*, vol. 2, nos. 2–4, pp. 209–239, Aug. 2008.
[38] K. Elamvazhuthi and S. Berman, "Mean-field models in swarm robotics: A survey," *Bioinspiration Biomimetics*, vol. 15, no. 1, Nov. 2019, Art. no. 015001.
[39] H. Hamann and T. Schmickl, "Modelling the swarm: Analysing biological and engineered swarm systems," *Math. Comput. Model. Dyn. Syst.*, vol. 18, no. 1, pp. 1–12, Feb. 2012.
[40] E. N. Gilbert, "Random plane networks," *J. Soc. Ind. Appl. Math.*, vol. 9, no. 4, pp. 533–543, Dec. 1961.
[41] C. P. Dettmann and O. Georgiou, "Random geometric graphs with general connection functions," *Phys. Rev. E, Stat. Phys. Plasmas Fluids Relat. Interdiscip. Top.*, vol. 93, no. 3, Mar. 2016, Art. no. 032313.
[42] M. Penrose, *Random Geometric Graph*. New York, NY, USA: Oxford Univ. Press, 2003.
[43] I. Stojmenovic, "Position-based routing in ad hoc networks," *IEEE Commun. Mag.*, vol. 40, no. 7, pp. 128–134, Jul. 2002.
[44] M. Mauve, J. Widmer, and H. Hartenstein, "A survey on position-based routing in mobile ad hoc networks," IEEE Netw., vol. 15, no. 6, pp. 30–39, Nov. 2001.
[45] M. Dorigo, E. Bonabeau, and G. Theraulaz, "Ant algorithms and stigmergy," *Future Gener. Comput. Syst.*, vol. 16, no. 8, pp. 851–871, Jun. 2000.
[46] D. L. Applegate, *The Traveling Salesman Problem: A Computational Study*, vol. 4. Princeton, NJ, USA: Princeton Univ. Press, 2006.
[47] S. Steinerberger, "New bounds for the traveling salesman constant," *Adv. Appl. Probab.*, vol. 47, no. 1, pp. 27–36, Mar. 2015.
[48] C. L. Valenzuela and A. J. Jones, "Estimating the held-karp lower bound for the geometric TSP," *Eur. J. Oper. Res.*, vol. 102, no. 1, pp. 157–175, Oct. 1997.
[49] M. Yang, Y. Tian, and X. Qi, "Behavior analysis of swarm robot systems based on vicsek model," in *Proc. 4th Int. Conf. Natural Comput.*, 2008, pp. 594–598.
[50] L. C. A. Pimenta, G. A. S. Pereira, N. Michael, R. C. Mesquita, M. M. Bosque, L. Chaimowicz, and V. Kumar, "Swarm coordination based on smoothed particle hydrodynamics technique," *IEEE Trans. Robot.*, vol. 29, no. 2, pp. 383–399, Apr. 2013.
[51] T. B. Apker and M. A. Potter, "Robotic swarms as solids, liquids and gasses," in *Proc. AAAI Fall Symp. Ser.*, 2012, pp. 8–13.
[52] M. Vigelius, B. Meyer, and G. Pascoe, "Multiscale modelling and analysis of collective decision making in swarm robotics," *PLoS ONE*, vol. 9, no. 11, Nov. 2014, Art. no. e111542.
[53] P. Atkins and J. de Paula, *Physical Chemistry for the Life Sciences*. Oxford, U.K.: Oxford Univ. Press, 2011.
[54] R. J. Hyndman and A. B. Koehler, "Another look at measures of forecast accuracy," *Int. J. Forecasting*, vol. 22, no. 4, pp. 679–688, Oct. 2006.
[55] W. K. V. Chan, "Interaction metric of emergent behaviors in agent-based simulation," in *Proc. Winter Simul. Conf. (WSC)*, Dec. 2011, pp. 357–368.
[56] B. Fraser, R. Hunjet, and C. Szabo, "Simulating the effect of degraded wireless communications on emergent behavior," in *Proc. Winter Simul. Conf. (WSC)*, Dec. 2017, pp. 4081–4092.
[57] J. C. Mogul, "Emergent (mis)behavior vs. complex software systems," in *Proc. 1st ACM SIGOPS/EuroSys Eur. Conf. Comput. Syst.* New York, NY, USA: ACM, 2006, pp. 293–304.
[58] B. Krishnamachari, S. B. Wicker, and R. Bejar, "Phase transition phenomena in wireless ad hoc networks," in *Proc. GLOBECOM. IEEE Global Telecommun. Conf.*, vol. 5, Nov. 2001, pp. 2921–2925.

BRADLEY FRASER received the B.Sc. degree (Hons.) in astrophysics from Macquarie University, in 2007, and the Graduate Certificate in defence science from The University of Adelaide, in 2014, where he is currently pursuing the Ph.D. degree, investigating emergent behavior and heuristic algorithms for the control of autonomous UAS swarms to provide data ferrying services in disconnected tactical networks, force projection and information, and surveillance and reconnaissance in the battlespace. He is also a Senior Research Engineer with the Defence Science and Technology Group. Since joining their Survivable Networks Group, in 2010, he has developed field-tested networked autonomous systems for wireless tactical networks. He is also a member of the Aerial Autonomous Systems Group, and his research involves the development of cooperative teaming behavior for uninhabited aircrafts using multiagent reinforcement learning algorithms.

ANDREW COYLE received the degree (Hons.) and Ph.D. degree in applied mathematics from The University of Adelaide. He has over 25 years of experience in mathematical modeling. He has worked in diverse areas, such as forestry, hydrology, power generation, and image processing. He joined the Centre for Defence Communications Information Networking as a Senior Research Fellow, in July 2001, and took up the position of the Deputy Director, in January 2002. He has worked on diverse communications projects such as the Video to the Bunk Project that investigated Australian Collins class submarines using a COTS wireless network. He has also analyzed tactical data links networks, various MANET routing protocols, the use of UAS to improve tactical network performance, and underwater communications for mine clearing autonomous vehicles.

ROBERT HUNJET received the Ph.D. degree from The University of Adelaide, in 2012. His Ph.D. thesis was on the use of autonomy to enable adaptive network topologies. He has been working with Defence Science and Technology Group, Australia, since 2001. He is the Group Leader of their Advanced Vehicle Systems Science and Technology Capability and an Adjunct Associate Professor with the School of Engineering and Information Technology, UNSW Canberra. He is also the Co-Lead of the Networked Land Autonomy Theme, Defence Collaborative Research Centre on Trusted Autonomous Systems. He leads a research team that seeks to enable autonomy through distributed control of sensors and effectors across federated land vehicles. His research interests are wireless network performance, swarming and emergence, autonomous decision-making, network survivability, and distributed control.

CLAUDIA SZABO is currently an Associate Professor with the School of Computer Science and the Director of the Complex Systems Research Group, The University of Adelaide. Her researches focus on modeling and analysis of complex systems, and practical applications of complexity theory and emergent behavior identification approaches to various application domains.